Gd^{3+}-Based Magnetic Resonance Imaging Contrast Agent Responsive to Zn^{2+}

Martín Regueiro-Figueroa[a], Serhat Gündüz[b], Véronique Patinec[c], Nikos K. Logothetis[d,e], David Esteban-Gómez[a], Raphaël Tripier[c], Goran Angelovski[*b], and Carlos Platas-Iglesias[*a]

[a] Grupo QUICOOR, Centro de Investigaciones Científicas Avanzadas (CICA) and Departamento de Química Fundamental, Universidade da Coruña, Campus da Zapateira, Rúa da Fraga 10, 15008 A Coruña, Spain

[b] MR Neuroimaging Agents, Max Planck Institute for Biological Cybernetics, Spemannstr. 41, 72076 Tübingen, Germany

[c] UFR des Sciences et Techniques, Université de Bretagne Occidentale, UMR-CNRS 6521, 6 avenue Victor le Gorgeu, C.S. 93837, 29238 BREST Cedex 3, France

[d] Physiology of Cognitive Processes, Max Planck Institute for Biological Cybernetics, Tübingen, Germany

[e] Department of Imaging Science and Biomedical Engineering, University of Manchester, Manchester, U.K.

Inorganic Chemistry Volume 54, Issue 21, pages 10342–10350, October 15, 2015
Received: 30 July 2015, Published online: 15 October 2015, Published in print: 2 November 2015

How to cite:

Gd3+-Based Magnetic Resonance Imaging Contrast Agent Responsive to Zn2+. Martín Regueiro-Figueroa, Serhat Gündüz, Véronique Patinec, Nikos K. Logothetis, David Esteban-Gómez, Raphaël Tripier, Goran Angelovski, and Carlos Platas-Iglesias. *Inorganic Chemistry* **2015** *54* (21), 10342-10350
DOI: 10.1021/acs.inorgchem.5b01719

Abstract

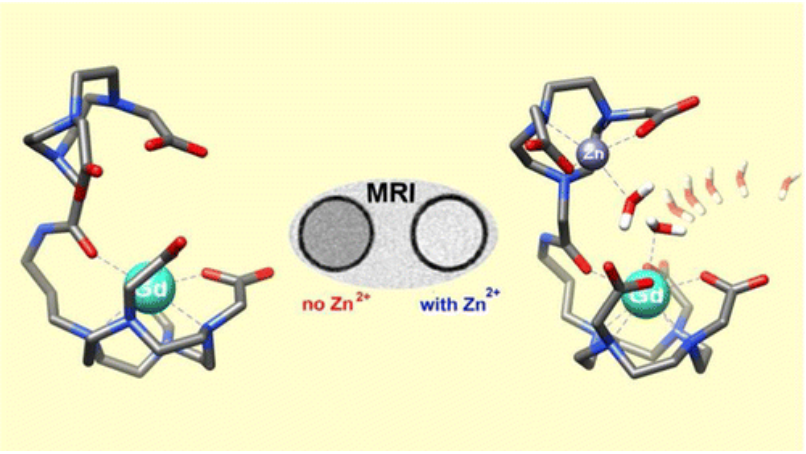

We report the heteroditopic ligand H_5L, which contains a DO3A unit for Gd^{3+} complexation connected to an NO2A moiety through a *N*-propylacetamide linker. The synthesis of the ligand followed a convergent route that involved the preparation of 1,4-bis(*tert*-butoxycarbonylmethyl)-1,4,7-triazacyclononane following the orthoamide strategy. The luminescence lifetimes of the Tb($^5D_4$) excited state measured for the TbL complex point to the absence of coordinated water molecules. Density functional theory calculations and ^1H NMR studies indicate that the EuL complex presents a square antiprismatic coordination in aqueous solution, where eight coordination is provided by the seven donor atoms of the DO3A unit and the amide oxygen atom

of the *N*-propylacetamide linker. Addition of Zn^{2+} to aqueous solutions of the TbL complex provokes a decrease of the emission intensity as the emission lifetime becomes shorter, which is a consequence of the coordination of a water molecule to the Tb^{3+} ion upon Zn^{2+}binding to the NO2A moiety. The relaxivity of the GdL complex recorded at 7 T (25 °C) increases by almost 150% in the presence of 1 equiv of Zn^{2+}, while Ca^{2+} and Mg^{2+} induced very small relaxivity changes. In vitro magnetic resonance imaging experiments confirmed the ability of GdL to provide response to the presence of Zn^{2+}.

Keywords: contrast agents; coordination compounds; gadolinium; lanthanides; NMR imaging

Introduction

Zn^{2+} is one of the most abundant metal ions in the human body that plays a critical role acting as a structural component of many proteins or the active site of enzymes.[1] Most of the Zn^{2+} present in the body is tightly bound in proteins, and thus the concentration of free Zn^{2+} in serum is relatively low (~15–20 μM).[2] However, mobile Zn^{2+} is present at particularly high concentrations in certain organs such as brain, pancreas and prostate, where it plays important physiological roles.[3] In the case of brain, chelatable Zn^{2+} is involved in the regulation of neuronal transmission, but both zinc overload and deficiency induce susceptibility to apoptosis.[4] Failures in homeostasis of mobile Zn^{2+} have been also associated with different neurological diseases such as ischemia, epilepsy, Parkinson's disease or Alzheimer's disease.[5] A class of glutamatergic neurons found mainly in the neo-cortex and limbic structures are susceptible to accumulate Zn^{2+} at high concentrations (~1 mM). High concentrations of Zn^{2+} have been observed in the neo-cortex of Alzheimer's disease patients together with amyloid deposits, which suggested that the amyloid pathology of Alzheimer's disease arises from Zn^{2+} release during glutamatergic neurotransmission events.[6] Thus, the development of probes to detect Zn^{2+} in biological systems is of great importance to shed light on the biological processes (pathological or not) mediated by this metal ion.[7]

Magnetic resonance imaging (MRI) is a technique widely used by radiologists that is particularly well-suited for obtaining high-resolution images of soft tissues. MRI uses the ^{1}H NMR signal of water molecules present in the body to generate contrast taking advantage of differences in the density of protons or the longitudinal (T_1) and transverse (T_2) relaxation times.[8] Image contrast may be improved with the administration of contrast agents (CAs), often Gd^{3+} complexes that contain at least one water molecule coordinated to the metal ion exchanging rapidly with the bulk water of the body.[8,9] These paramagnetic compounds provide an efficient mechanism for the longitudinal and transverse relaxation enhancement ($1/T_1$ and $1/T_2$) of water protons, which is translated into image contrast. Responsive or smart CAs are a subclass of these paramagnetic probes capable of changing the T_1 and/or T_2 as a function of certain physiological parameters.[10] Many responsive agents have been reported in the past years that are sensitive to temperature,[11] pH,[12] redox activity,[13] enzymatic activity,[14] or biologically relevant ions.[15] Among these, a number of Zn-responsive agents with great structural variety were studied. Most commonly, a well-known and selective chelator *N*,*N*-bis(2-pyridyl-methyl) ethylene diamine (BPEN) was coupled to DTPA,[16] DOTA,[17,18] or porphyrins[19] to result in potent Zn sensors. Alternatively, Zn^{2+} chelators consisting of substituted diacetateamine[20] or sulfonamidoquinoline[21] fragments, a bis(pyridinylmethyl)amine unit[22] or an amidoquinoline moiety[23] coupled to DO3A or polyamino polycarboxylates containing pyridine moieties as Gd^{3+}-chelators were also used.

In spite of the variety of Zn^{2+}-responsive Gd^{3+}-based CAs reported in the literature, some of their features are still to be improved. First, the relatively fast dissociation kinetics of Gd^{3+}-DTPA complexes in vivo represents an important drawback of the first generation of responsive probes based on DTPA,[16] as dissociation of the complex with Gd^{3+} release may result in undesirable side effects.[24,25] Second, MRI has the intrinsic disadvantage of its low sensitivity compared to other techniques such as fluorescence.[17a] The

reported Zn^{2+}-responsive MRI probes provide responses that fall typically within the range of 20–70% in terms of the relaxivity changes induced by the presence of Zn^{2+},[16-23] although a relaxivity change of up to 165% has been reported for a Zn^{2+} probe in the presence of human serum albumin (HSA).[17c] However, improving the response of this kind of probes is highly desirable to improve the sensitivity and/or reduce the doses of paramagnetic agent to be injected. Third, several of the CAs responsive to Zn^{2+} present an optimal response at low fields (20–60 MHz),[17,20b,22] while higher spatial resolution and better sensitivity is currently stimulating the development of high-field (3 T) and ultrahigh field (>3 T) MRI scanners.[26]

Our groups were also involved in the development of responsive agents. A series of Gd^{3+}complexes with mono- (H_5L^1, Chart 1) and bis-macrocyclic (H_8L^2–H_8L^3) ligands providing selective and strong relaxivity response for Ca^{2+} over Mg^{2+} were reported by Angelovski et al.[28,27] Besides the evaluation of the complex in vitro,[29] their nanosized analogues were recently tested in vivo, exhibiting very advantageous properties.[30,31] These systems contain one or two DO3A units for Gd^{3+} complexation, which are coupled to a non-macrocyclic Ca^{2+}-binding moiety via an amide bond. This amide group is also involved in the coordination to Gd^{3+},[25] thus making the whole system prone to easy coordination and thus the relaxivity changes. Consequently, the number of water molecules coordinated to Gd^{3+} increases in the presence of Ca^{2+}, provoking a relaxivity increase and thus MRI response. Furthermore, the same structural motif was coupled to the aza-crown containing Gd^{3+} complexes, resulting in the series of neurotransmitter-sensitive contrast agents.[32]

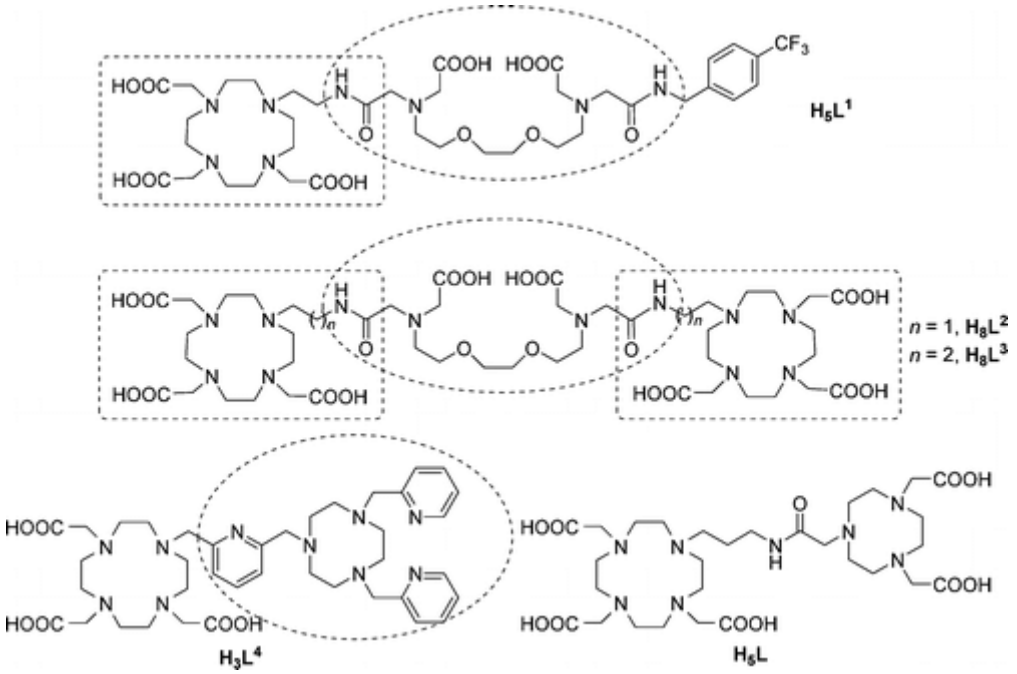

Chart 1. Chemical Structure of the Ligands Discussed in This Work[a]

However, a ligand H_3L^4, which contains a TACN moiety introduced for Zn^{2+} sensing purposes, was recently reported by Platas-Iglesias and Tripier et al.[33] However, Zn^{2+} addition did not provoke a change in the number of water molecules coordinated to Gd^{3+}, although turn-on behavior of the ligand-centered luminescence was induced by Zn^{2+}. Obviously, an appropriate nature of the Gd^{3+} chelator (DO3A unit) and the linker is needed to result in the potential contrast agent that will respond to the external stimulus (e.g.,

[a] The dashed rectangles indicate the structural motif responsible for relaxivity changes in responsive CAs, while the dashed ellipsoids highlight the Ca^{2+}- or Zn^{2+}-binding motifs used in previous studies.

change in Zn^{2+} concentration) by changing the relaxivity. Therefore, we sought to combine the successfully used responsive part with a Zn^{2+}chelator. Thus, herein we report the heteroditopic ligand H_5L, which contains a DO3A unit for Gd^{3+}complexation linked by the same *N*-propylacetamide moiety to a NO2A moiety for Zn^{2+} binding. The GdL complex was assessed as a Zn^{2+}-responsive MRI probe by using different spectroscopic and computational techniques.

Results and Discussion

Ligand Synthesis

The synthesis of 1,7-bis(*tert*-butoxycarbonylmethyl)-1,4,7-triazacyclononane **5** was performed using a benzylation/dialkylation/debenzylation sequence (Scheme 1). Reaction of 1,4,7-triazacyclononane (TACN) with *N*-dimethoxymethyl-*N*,*N*-dimethylamine gave rise to the formation of the already known orthoamide 1,4,7-triazatricyclo[5.2.1.$0^{4,10}$]decane **1**, which has been shown to be an efficient intermediary in the monoalkylation of TACN with halogenoalkane derivatives.[34] Addition of benzyl bromide to **1** resulted in the precipitation of the corresponding ammonium salt **2** as a white powder. Acidic hydrolysis with HCl 12 M/methanol (1/1) and further basic treatment gave the deprotected benzyl derivative **3** with 90% overall yield. Alkylation of the two remaining secondary amine functions proceeded in acetonitrile in the presence of an excess of K_2CO_3 by using 1.8 equiv of *tert*-butyl bromoacetate in order to favor the dialkylated product **4** instead of the quaternarization of nitrogen atoms. Derivative **4** was obtained with 63% yield after purification by column chromatography. Removal of the benzyl arm in the last step was performed under H_2pressure with Pd/C (10%) in absolute ethanol to produce compound **5** (NO2A*t*Bu) in 76% yield. This secondary amine was then alkylated with the bromomethyl derivative **6**[28] that carries the responsive DO3A moiety using K_2CO_3 as the base to give the bismacrocyclic compound **7**. The desired chelator H_5L was finally obtained by hydrolysis of *tert*-butyl esters in trifluoroacetic acid at room temperature (RT).

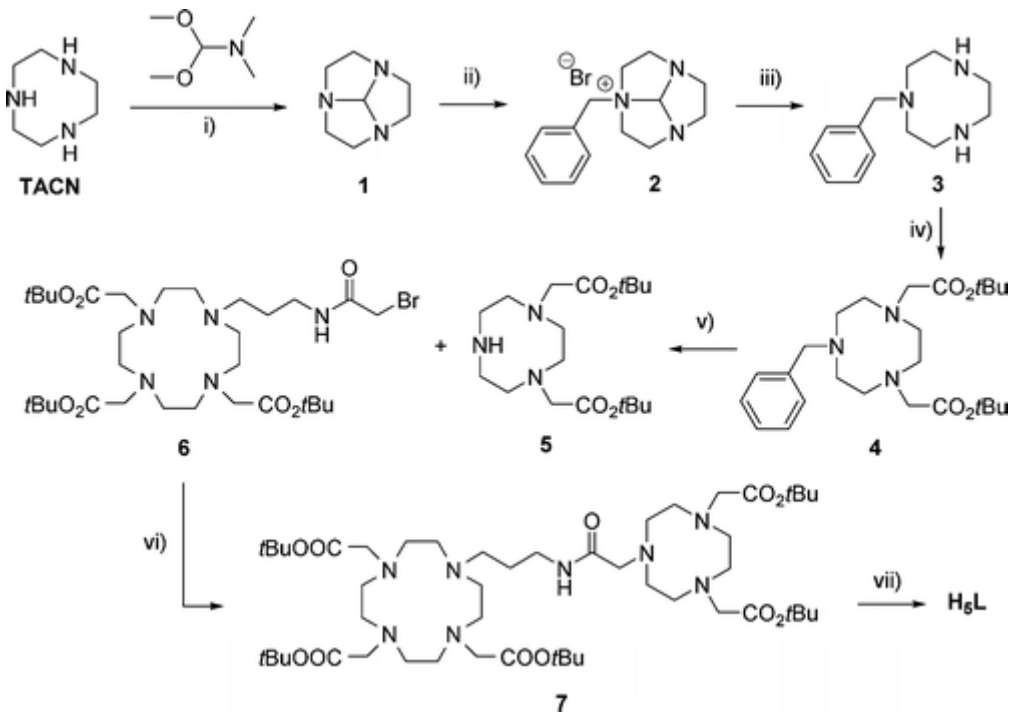

Scheme 1. Synthesis of H_5L[a]

Complexation Studies

To avoid problems arising from the formation of binuclear lanthanide complexes or the presence of free ligand, the stock solution of the ligand used for the preparation of the LnL complexes was standardized by titration with $CuSO_4 \cdot 5H_2O$ in acetate buffer (pH 5.8, Figure S1, Supporting Information). Addition of Cu^{2+} to a solution of the ligand results in the formation of a broad and weak absorption band at 725 nm attributed to d–d transitions. The titration profile shows a sharp inflection point that signals a 1:2 stoichiometry (L/Cu), pointing to the formation of a binuclear Cu^{2+}complex. Addition of an excess of metal ion causes a red shift of the absorption band to 742 nm due to the formation of the Cu^{2+} aqua ion.

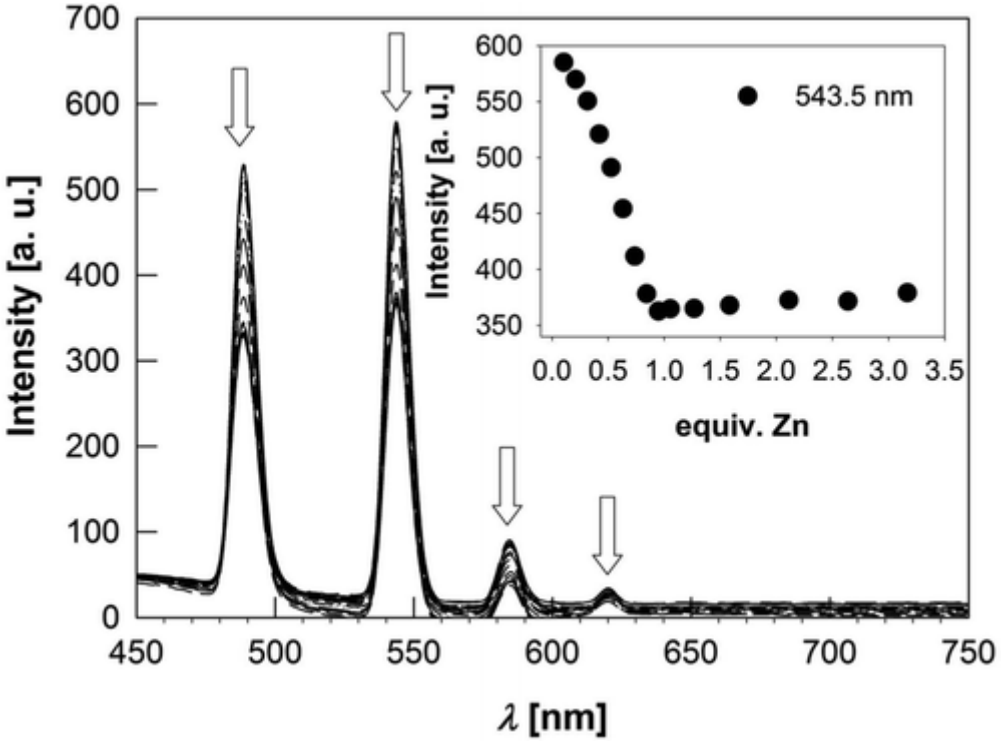

Figure 1. Emission spectra taken during the course of the titrations of a 1 mM solution of TbL (λ_{exc} = 230.5 nm) with a standard solution of $Zn(CF_3SO_3)_2$ ca. 53 mM in aqueous solution at pH 7.4 (0.1 M MOPS buffer).

The GdL and TbL complexes were prepared by reacting equimolar amounts of the H_5L ligand and $LnCl_3 \cdot 6H_2O$ salts in aqueous solution at pH 5.8 and 80 °C for 24 h. The high-resolution mass spectra (ESI^+) of the aqueous solutions of the GdL and TbL complexes show peaks due to the $[GdNa_2HL]^+$ and $[NaTbH_2L]^+$ entities, which indicates the formation of the mononuclear complexes (Figures S2 and S3, Supporting Information). The emission spectrum of the TbL complex recorded upon excitation at 230.5 nm shows weak luminescence due to the $^5D_4 \rightarrow {}^7F_J$ transitions characteristic of Tb^{3+} (488 nm, J = 6; 543 nm, J = 5; 583 nm, J = 4; 618 nm, J = 3, Figure 1). The excited-state lifetimes of the TbL complex were measured in water (τ_{H2O} = 2.22 ms) and deuterated water (τ_{D2O} = 2.63 ms), which allows estimating the number of water molecules in the first coordination sphere of the metal ion according to the methodology developed by Horrocks,[35] using the refined coefficients determined by Parker et al.[36] These emission lifetimes provide a hydration number q = 0.05, which points to the absence of water molecules coordinated to the Tb^{3+} ion in aqueous solution. Both the DO3A and NO2A moieties of the ligand can in principle form stable complexes with the Ln^{3+} ions in aqueous solutions. However, the stability constant of the [Gd(NOTA)] complex (H_3NOTA = 1,4,7-triazacyclononane-1,4,7-triacetic acid, $\log K_{GdL}$ = 14.4)[37] is 7 orders of magnitude lower than that of [Gd(DO3A)] (H_3DO3A = 1,4,7,10-tetraazacyclododecane-1,4,7-triacetic acid,

log K_{GdL} = 21.0),[38] and thus the Ln^{3+} ions in LnL complexes are expected to be coordinated to the DO3A unit, provided that the thermodynamic equilibrium is attained. The hydration number determined from luminescence lifetime measurements suggests that the Ln^{3+} ion is coordinated by the DO3A unit of the ligand, as [Ln(NOTA)] complexes were reported to have 2–4 coordinated water molecules.[39] The absence of coordinated water molecules is in line with the results obtained by Parker et al. for complexes with a DO3A ligand containing a N-linked $CH_2CH_2CH_2NHCO$–pyridyl moiety.[40] Furthermore, the absence of inner-sphere water molecules points to the coordination of the amide oxygen atom of the linker to the Ln^{3+} ion, as proposed by Parker and co-workers for Ln^{3+} complexes containing the same linker.[40] Coordination of the amide oxygen atoms was also proposed for related Ca^{2+}-sensitive probes on the basis of NMR data recorded for the Y^{3+} complex.[27] Indeed, the noncoordination of the amide oxygen atom would result in a coordination environment typical of DO3A derivatives, which contain at least a coordinated water molecule.[41]

The ^{1}H NMR spectrum of the EuL complex presents a large number of relatively broad paramagnetically shifted signals in the range from +25 to −20 ppm (Figure 2). In Eu^{3+} complexes of DOTA, DOTA–tetraamide, and DO3A derivatives the signals of the pseudo axial protons on the cyclen rings are usually found between 24 and 45 ppm in the square antiprismatic (SAP) isomer and below 20 ppm in the twisted-square antiprismatic (TSAP) isomer.[42] These protons are observed in the range from +15 to +25 ppm for EuL, and therefore an unequivocal assignment of the structure of the complex in solution is not possible in this case.

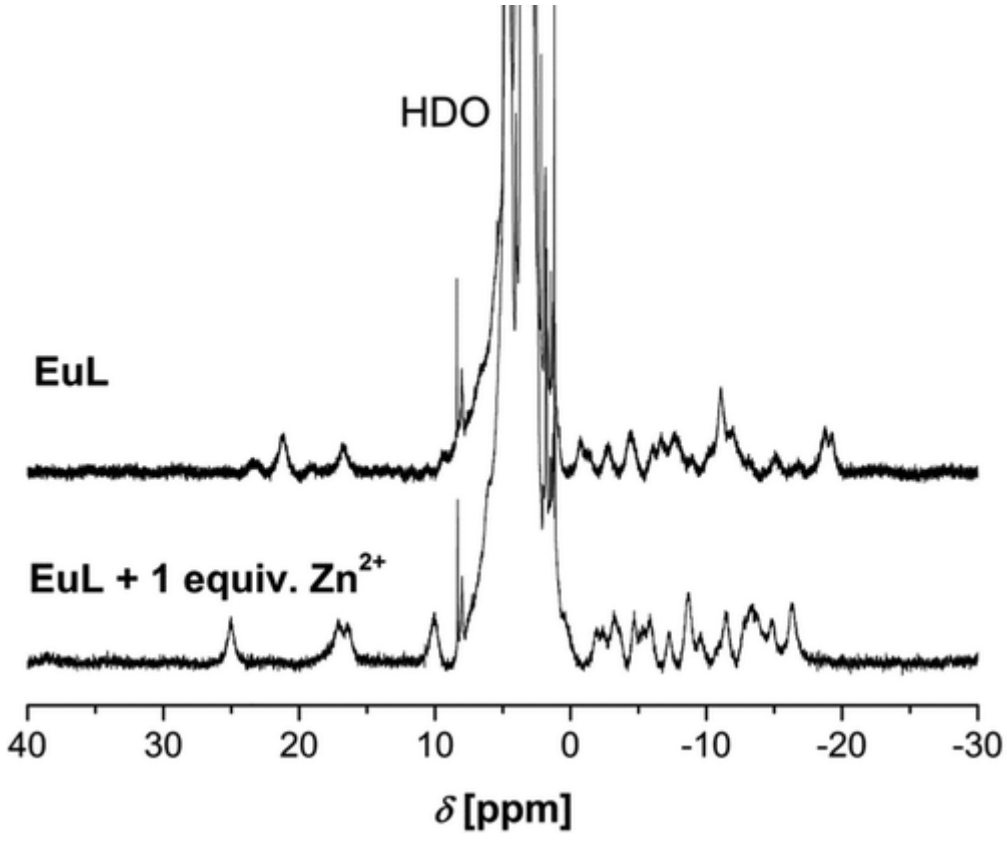

Figure 2. ^{1}H NMR spectra of EuL recorded in D_2O solution (pD = 7.0, 300 MHz, 25 °C) in the absence and in the presence of 1 equiv of Zn^{2+}.

The EuL and GdL complexes were investigated by means of density functional theory (DFT) calculations using the TPSSh functional and the large-core relativistic ECP of Dolg et al., following the methodology

reported in recent computational studies (see Computational details below).[29,43] Considering the protonation constants reported for TACN derivatives, this moiety is expected to be protonated at about neutral pH,[34] and therefore our calculations were performed on the $LnHL^+$ model systems (Ln = Eu or Gd). Geometry optimizations provided the expected SAP and TSAP isomers as minimum energy conformations. According to these computations the SAP isomer is more stable than the TSAP one, the free energy differences between the two forms being 10.3 (EuL) and 10.8 kJ mol^{-1} (GdL). Thus, most likely these complexes present an SAP coordination in aqueous solution (Figure 3). As expected due to their negative charge, the Gd–O distances involving oxygen atoms of carboxylate groups (2.33–2.35 Å) are shorter than the Gd–O amide distance (2.42 Å). Overall, the distances between the Gd^{3+} ion and the ligand donor atoms are in good agreement with those observed for complexes of this ion with different cyclen-based ligands.[9a] The protonated NO2A unit is placed above the GdDO3A entity, which likely prevents the coordination of a water molecule to the metal ion. This conformation appears to be stabilized by the presence of a hydrogen-bond involving the amide NH group and one of the nitrogen atoms of the NO2A moiety (Figure 3).

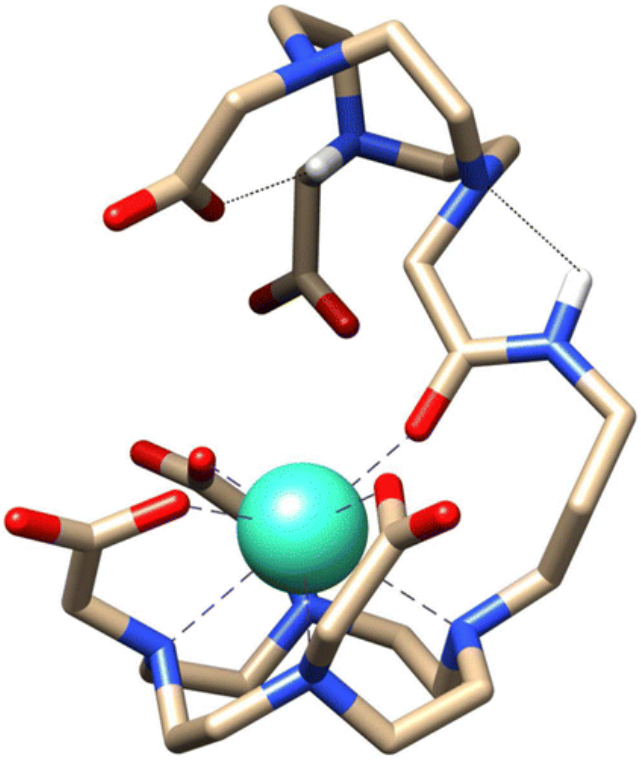

Figure 3. Optimized geometry of the SAP isomer of $GdHL^+$ obtained from DFT calculations (TPSSh/6-31G(d,p)). H atoms are omitted for simplicity, except those involved in hydrogen bonds.

Zn^{2+} Binding Studies

The high-resolution mass spectrometry (HR-MS) of an aqueous solution of TbL in the presence of equimolar Zn^{2+} presents a peak due to the $[NaTbZnL]^+$ entity, which demonstrates the formation of the heterodinuclear complex (Figure S4, Supporting Information). Addition of Zn^{2+} to an aqueous solution of TbL at pH 7.4 (0.1 M 3-(*N*-morpholino)propanesulfonic acid (MOPS) buffer) causes a decrease of the emission intensity due to the Tb^{3+}-centered $^5D_4 \rightarrow {}^7F_J$ transitions (Figure 1), with a sharp inflection point being observed upon addition of 1 equiv of Zn^{2+}. Addition of an excess of the divalent metal ion does not cause further changes in the emission intensity nor in the emission lifetime of the $^5D_4$ excited state. The emission lifetime decreases from 2.22 to 1.37 ms upon addition of 1 equiv of Zn^{2+} in H_2O solution. The emission lifetime recorded in D_2O

solution in the presence of Zn^{2+} was τ_{D2O} = 2.18 ms, which corresponds to a hydration number q = 1.07 as estimated by the relationship proposed by Parker.[33] This result points to an increase of the number of coordinated water molecules from 0 to 1 upon Zn^{2+} binding. This suggests that the amide oxygen atom of the linker connecting the cyclen and TACN fragments of the ligand remains coordinated to the Ln^{3+} ion, as Ln^{3+} DO3A derivatives often have hydration numbers close to two.[44] The ^{1}H NMR spectrum of the EuL complex (Figure 2) experiences only slight changes upon Zn^{2+} addition, which also supports that the coordination environment of the Ln^{3+}ion remains very similar. DFT calculations support this hypothesis, as they show that coordination of the amide group to the lanthanide ion and pentadentate coordination of Zn^{2+} to the NO2A moiety are feasible (Figure 4). Both metal ions are likely to complete coordination numbers 6 (for Zn^{2+}) and 9 (for Gd^{3+}) with the presence of a coordinated water molecule. Given that the amide oxygen atom is likely to be coordinated to the Gd^{3+} ion both in the absence and in the presence of Zn^{2+}, the driven force behind the hydration number increase observed upon Zn^{2+} binding is not obvious. We hypothesize that the increased positive charge of the system upon Zn^{2+} coordination is mainly responsible for this effect. The absence of coordinated water molecules in the case of the charge neutral DO3A complex of Parker and co-workers, which contains an amide group with the same linker as L,[40] together with the presence of a coordinated water molecule in a very similar Gd^{3+} complex that presents a positive charge,[32] are in line with this hypothesis.

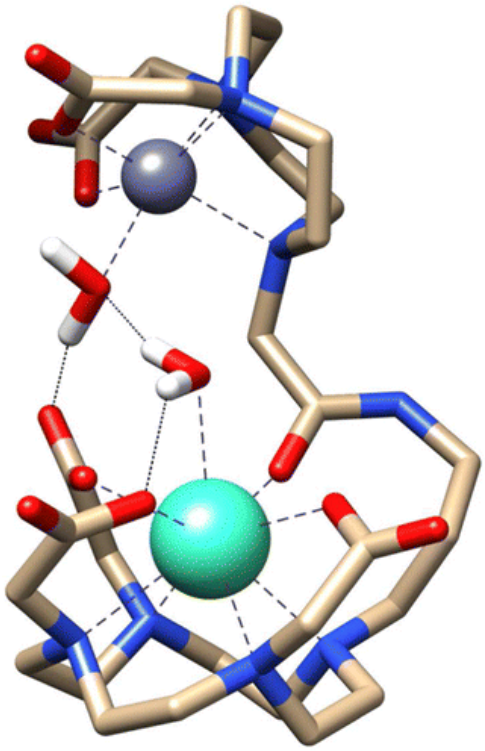

Figure 4. Optimized geometry of the SAP isomer of $GdZnL^{2+}$ obtained from DFT calculations (TPSSh/6-31G(d,p)). H atoms are omitted for simplicity, except those involved in hydrogen bonds.

The efficiency of a given paramagnetic complex as an MRI contrast agent is often assessed in vitro in terms of relaxivity, which is defined as the longitudinal relaxation rate enhancement of water proton nuclei per millimolar concentration of the paramagnetic probe. The relaxivity of GdL measured at 25 °C and 7 T amounts to 3.08 ± 0.08 mM^{-1} s^{-1}, a value that is compatible with the absence of inner sphere water molecules.[27,28] As a result, the observed relaxivity arises from the outer-sphere mechanism, which is related to the close diffusion of outer-sphere water molecules in the vicinity of the paramagnetic center. Addition of

Zn^{2+} induces a dramatic increase of the relaxivity, which reaches a value of 7.50 ± 0.08 mM^{-1} s^{-1} upon addition of 1 equiv of Zn^{2+}(Figure 5). This represents almost a 150% relaxivity increase, which can only be explained by the coordination of a water molecule to the Gd^{3+} ion, although a contribution of second-sphere water molecules to the overall relaxivity cannot be ruled out.[45] The relaxivity measured in the presence of 1 equiv of Zn^{2+} is very similar to those reported for related Ca^{2+}- and neurotransmitter-sensitive probes.[27,32] Furthermore, it is lower than those observed for Ca^{2+}-sensitive probes exhibiting second-sphere contribution to relaxivity.[45] In those cases, the hydration numbers were confirmed with luminescence measurements (using both Eu^{3+} and Tb^{3+}complexes) and extensive NMRD and ^{17}O NMR studies, which provided ^{17}O hyperfine coupling constants in agreement with monohydrated complexes.

The steep curvature of the titration profile around the 1:1 (GdL/Zn^{2+}) stoichiometry ratio is characteristic of an especially high association constant, preventing the determination of an accurate equilibrium constant.[46] Interestingly, addition of Ca^{2+} or Mg^{2+} instead of Zn^{2+} causes only slight relaxivity enhancements (16 and 6%, respectively), which shows that the GdL probe provides selective response for Zn^{2+} over the main competitors in vivo. In line with these results addition of Ca^{2+} or Mg^{2+} to the TbL complex provokes very minor changes in the luminescence emission intensity (Figure S5, Supporting Information). Furthermore, the stability constants reported for complexes of the TACN derivative NOTA show that the complex formed with Zn^{2+} is 8–9 orders of magnitude more stable than those formed with Ca^{2+} and Mg^{2+}, and thus the presence of these metal ions even in large excess is not expected to interfere with Zn^{2+} binding.[47] As expected, relaxivity studies show that Cu^{2+} induces a relaxivity response comparable to that of Zn^{2+} (Figure 5), while the $[Cu(NOTA)]^-$ complex was shown to be more stable than the Zn^{2+} analogue.[47] However, this is likely not an important drawback for Zn^{2+} sensing in vivo, given the very low concentration of Cu^{2+} ion the body.[48]

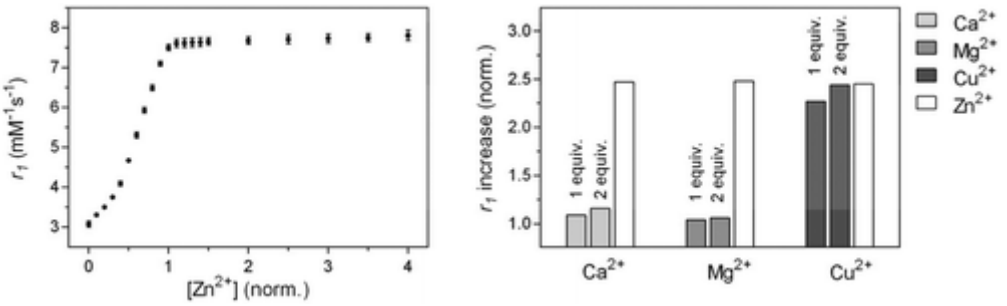

Figure 5. Relaxometric studies of GdL with endogenous cations. (left) Titration with Zn^{2+}. The r_1 values are represented as mean ± SD of three independent experiments and are normalized to $[Gd^{3+}]$ = 1 mM. (right) Competition experiments of Ca^{2+}, Mg^{2+}, or Cu^{2+} with Zn^{2+} in the presence of GdL (3 mM). Small SD values prevent visualization of error bars. In all cases the experiments were performed at 7 T magnetic field strength and pH 7.4 (HEPES).

The relaxivity enhancement observed for GdL in the presence of Zn^{2+} was further investigated by performing MRI experiments with tube phantoms (Figure 6) under the same conditions as in the relaxometric studies (7 T, pH 7.4, HEPES). For the sake of comparison, MRI experiments were also conducted using identical acquisition parameters and tubes with solution of GdDOTA and water as controls. In the absence of Zn^{2+}, GdL provides less contrast enhancement, almost comparable to GdDOTA ($r_1 \approx 3.9$ mM^{-1} s^{-1}).[49] Addition of Zn^{2+} to a solution of GdL provides a clear contrast enhancement, while the presence of Zn^{2+} does not provoke any contrast change in the solution of GdDOTA. Finally, no contrast enhancement was observed in tubes that did not contain any of the Gd^{3+} complexes but only water, either in absence or presence of Zn^{2+}. The signal-to-noise ratios (SNR) calculated for the solutions of GdL in the absence and in the presence of Zn^{2+} confirm the contrast enhancement (Figure 6).

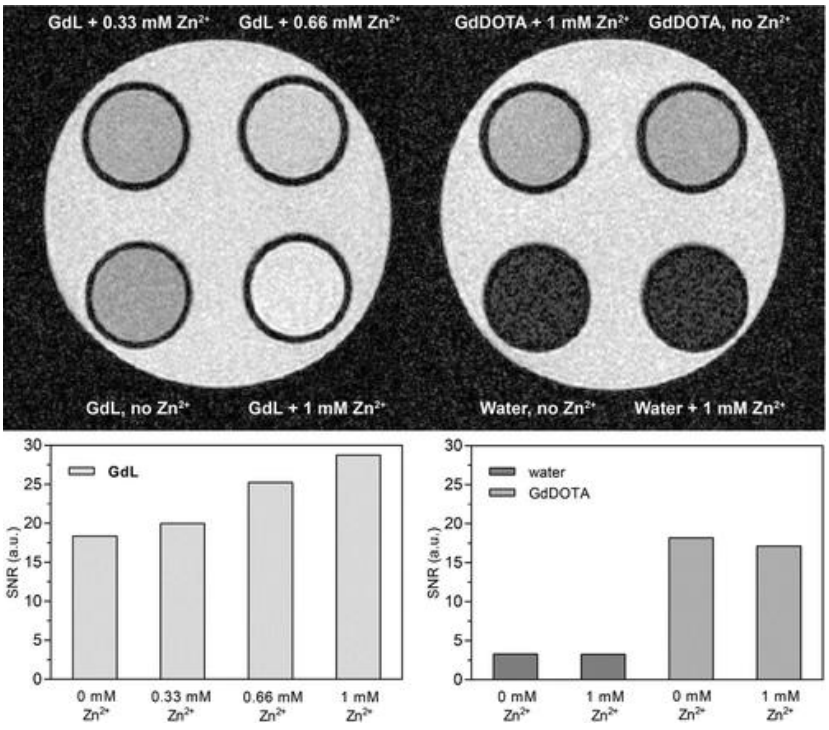

Figure 6. T_1-weighted MR images obtained from the imaging scanner operating at 7 T magnetic field. (left) Solutions of GdL (1 mM) mixed with different concentrations of Zn^{2+} at pH 7.4 (HEPES). (right) Control experiments with GdDOTA (1 mM, pH 7.4, HEPES) or water in absence or presence of Zn^{2+} (1 mM). The graphs placed below the MR images show the SNR calculated for each of the solutions.

Conclusions

In this work we have reported the synthesis of a heteroditopic ligand that yields a MRI contrast agent responsive to Zn^{2+} upon Gd^{3+} complexation. A combined study including luminescence lifetime measurements, ^{1}H NMR spectroscopy, and DFT calculations indicates octadentate coordination of the ligand to Gd^{3+} in GdL, which lacks inner-sphere water molecules. Coordination of Zn^{2+} to the TACN unit of the ligand triggers the coordination of a water molecule to Gd^{3+}, resulting in a 150% relaxivity enhancement at 7 T and 25 °C. This represents, to the best of our knowledge, the highest relaxivity response to Zn^{2+} of a Gd^{3+} probe at high field, although relaxivity changes as high as 200% have been reported at lower fields.[20b] Furthermore, Ca^{2+} and Mg^{2+}provoke very small relaxivity changes, showing that GdL provides a selective response toward Zn^{2+} over their main competitors. MRI studies in vitro confirmed the ability of GdL to provide remarkable response to Zn^{2+} in terms of an enhanced contrast.

Experimental and Computational Section

General Methods

Reagents were purchased from commercial sources unless otherwise specified. 1,4,7-Triazacyclononane was purchased from CheMatech (Dijon, France). Acetonitrile, tetrahydrofuran (THF), toluene, and chloroform were distilled before use. Compound **6** was synthesized according to previously published procedure.[28] ESI-TOF mass spectra were recorded using a LC-Q-q-TOF Applied Biosystems QSTAR Elite spectrometer or a MAXis 4G, Bruker Daltonics Inc, Germany, using both the positive and negative modes. High-resolution

mass spectra were recorded on a Bruker Daltonics APEX II (FT-ICR-MS) with an ESI source. UV–vis spectra were recorded on a PerkinElmer Lambda 900 spectrophotometer in 1.0 cm path quartz cells. Excitation and emission spectra were recorded on a PerkinElmer LS-50B spectrometer. Luminescence lifetimes were calculated from the monoexponential fitting of the average decay data, and they are averages of at least 3–5 independent determinations. ^{1}H and ^{13}C NMR spectra of organic molecules were recorded with a Bruker AMX-3 300 (300 MHz) or a Bruker Avance III 300 MHz spectrometer. ^{1}H NMR spectra of the EuL complex were recorded at 25 °C on a Bruker Avance 300 MHz spectrometer. Relaxometric titrations were performed using a Bruker Avance III 300 MHz spectrometer. Magnetic resonance imaging experiments at field strength of 7 T were performed on a BioSpec 70/30 USR magnet using Bruker quadrature volume coil (RF RES 300 1H 112/86 QSN TD AD).

1-Benzyl-[1,4,7]-triazacyclononane (3)

N-Dimethoxymethyl-*N*,*N*-dimethylamine (670 mg, 5.60 mmol, 1.1 equiv) was added to a solution of TACN (660 mg, 5.10 mmol) in chloroform (1 mL) and toluene (10 mL). The solution was stirred at RT for 12 h. The solvent was then evaporated under reduced pressure to yield an oily product. Benzyl bromide (1.1 equiv, 5.62 mmol, 670 μL) in solution in 15 mL of freshly distilled THF was added to the previous crude product. The precipitated white solid was filtered after the mixture was stirred at RT for 3 d, washed with THF, and dried under vacuum. The white solid was dissolved in 10 mL of a solution of methanol/HCl 12 M (1:1) and stirred at reflux for 12 h. After it cooled, the pH was raised to 12 by addition of NaOH pellets. Extraction with chloroform (3 × 15 mL), drying with $MgSO_4$, and evaporation of the solvent under reduced pressure gave the 1-benzyl-1,4,7-triazacyclononane **3** as a yellow oil (1.01g, 4.60 mmol, 90%). ^{1}H NMR (300 MHz, $CDCl_3$): δ 2.53 (m, 8H, C*H*$_{2TACN}$), 2.80 (s, 4H, C*H*$_{2TACN}$), 3.07 (s, 2H, N*H*), 3.60 (s, 2H, C*H*$_2$Ph), 7.12–7.23 (m, 5H, C_6H_5). ^{13}C NMR (75 MHz, $CDCl_3$): δ 46.1, 46.2, 52.3, 61.2, 126.7, 127.9, 128.6, 139.2.

(4-Benzyl-7-tert-butoxycarbonylmethyl-[1,4,7]-triazonan-1-yl)-acetic acid *tert*-butyl ester (4)

Compound **3** (1.01g, 4.60 mmol) was dissolved in 15 mL of freshly distilled acetonitrile, and 1.8 equiv of *tert*-butyl bromoacetate (1.61 g, 8.28 mmol) and K_2CO_3 (excess) were added. After it was stirred at RT for 4 d, the solution was filtered. Evaporation of the solvent gave an oily crude product. Purification was performed by chromatography on silica gel (elution with hexanes/$CHCl_3$2:1, R_f = 0.7). Compound **4** was obtained as a clear oil (1.30 g, 2.90 mmol, 63%). ^{1}H NMR (300 MHz, $CDCl_3$): δ 1.42 (s, 18H, C(C*H*$_3$)$_3$), 2.78 (bs, 4H, C*H*$_{2TACN}$), 2.81 (bs, 4H, C*H*$_{2TACN}$), 2.92 (s, 4H, C*H*$_{2TACN}$), 3.28 (s, 4H, C*H*$_2$CO$_2$*t*Bu), 3.65 (s, 2H, C*H*$_2$Ph), 7.14–7.32 (m, 5H, C_6H_5). ^{13}C NMR (75 MHz, $CDCl_3$): δ 28.2, 55.2, 55.3, 55.6, 59.9, 62.6, 80.4, 126.6, 128.0, 128.9, 140.2, 171.4.

(4-*tert*-Butoxycarbonylmethyl-[1,4,7]-triazonan-1-yl)-acetic acid *tert*-butyl ester (5): NO2A^{t}Bu

Compound **4** (1.30 g, 2.90 mmol) was dissolved in absolute ethanol, and 10% Pd/C activated was added. The reaction mixture was left under hydrogen atmosphere at RT under stirring for 4 d. After filtration through Celite, ethanol was removed by evaporation at reduced pressure to produce **5** as a yellow oil (790 mg, 2.21 mmol, 76%). ^{1}H NMR (300 MHz, $CDCl_3$): δ 1.40 (s, 18H, C(C*H*$_3$)$_3$), 2.71 (s, 4H, C*H*$_{2TACN}$), 3.01 (m, 4H, C*H*$_{2TACN}$), 3.19 (m, 4H, C*H*$_{2TACN}$), 3.32 (s, 4H, C*H*$_2$CO$_2$*t*Bu). ^{13}C NMR (75 MHz, $CDCl_3$): δ 28.1, 44.5, 49.2, 51.9, 56.7, 81.8, 170.7.

(4-{3-[2-(4,7-Bis-*tert*-butoxycarbonylmethyl-[1,4,7]-triazonan-1-yl)-acetylamino]-propyl}-7,10-bis-*tert*-butoxycarbonylmethyl-1,4,7,10-tetraaza-cyclododec-1-yl)-acetic acid *tert*-butyl ester (7)

The bromide **6** (750 mg, 1.05 mmol) was dissolved in acetonitrile (5 mL) and added slowly to the suspension of the azamacrocycle **5** (320 mg, 0.90 mmol) and potassium carbonate (371 mg, 2.69 mmol) in acetonitrile (20 mL). The reaction mixture was stirred at 70 °C for 16 h. After it cooled, the mixture was filtered, and the solvent was evaporated under reduced pressure. The residue was purified using column chromotography

(silica gel, 5% methanol/dichloromethane, R_f = 0.3) to give compound **7** as a light brown solid (330 mg, 0.34 mmol, 38%). ^{1}H NMR (300 MHz, $CDCl_3$): δ 1.41 (s, 9H, C*H*$_3$), 1.42 (s, 18H, C*H*$_3$), 1.48 (s, 18H, C*H*$_3$), 1.77 (br, 2H, C*H*$_2$), 1.95−3.73 (br, 42H, C*H*$_2$), 4.10 (s, 2H, C*H*$_2$), 9.02 (s, 1H, N*H*). ^{13}C NMR (75 MHz, $CDCl_3$): δ 24.3, 27.3, 27.5, 27.7, 37.2, 48.3, 50.0, 51.4, 51.7, 52.9, 55.2, 56.0, 56.4, 81.5, 82.1, 82.4, 169.3, 169.5, 171.0, 173.0. ESI-HRMS (*m*/*z*): $[M + H]^+$ calcd. for $C_{49}H_{93}N_8O_{11}^+$, 969.6958, found 969.6950, $[M + Na]^+$ calcd. for $C_{49}H_{92}N_8NaO_{11}^+$, 991.6778, found 991.6768.

(4-{3-[2-(4,7-Bis-carboxymethyl-[1,4,7]triazonan-1-yl)-acetylamino]-propyl}-7,10-bis-carboxymethyl-1,4,7,10-tetraaza-cyclododec-1-yl)-acetic acid (L)

Compound **7** (0.33 mmol, 300 mg) was dissolved in anhydrous dichloromethane (5 mL), and the solution was cooled to 0 °C. Trifluoroacetic acid (TFA; 5 mL) was slowly added, and the solution was stirred at RT for 16 h. The reaction mixture was concentrated under reduced pressure, and the residue was dissolved in a small portion of methanol. The product was precipitated from diethyl ether, isolated by decantation, and dried under reduced pressure to give $H_5L{\cdot}5CF_3COOH$ as a pale brown hygroscopic solid (300 mg, 73%). ^{1}H NMR (300 MHz, D_2O): δ 1.84−2.03 (br, 2H, C*H*$_2$), 2.73−4.13 (br, 44H, C*H*$_2$). ^{13}C NMR (75 MHz, D_2O): δ 23.2, 35.9, 36.6, 48.6, 48.9, 49.5, 49.9, 50.7, 51.3, 51.9, 53.3, 53.5, 55.7, 56.6, 58.9, 60.9, 116.3 (TFA), 162.9 (TFA), 169.8, 172.7, 172.8, 174.1, 175.1. ESI-HRMS (*m*/*z*): $[M + H]^+$ calcd. for $C_{29}H_{53}N_8O_{11}^+$, 689.3828, found 689.3830.

Computational Details

All calculations reported in this work were performed employing the Gaussian 09 package (Revision D.01).[50] Full geometry optimizations of the $LnHL^+$ and $LnZnL^{2+}$ systems were performed in aqueous solution employing DFT within the hybrid meta-generalized gradient approximation (hybrid meta-GGA), with the TPSSh exchange-correlation functional.[51] Geometry optimizations were performed by using the large-core quasirelativistic effective core potential of Dolg and coworkers and its associated [5s4p3d]-GTO valence basis set,[52] while the ligand atoms and Zn were described by using the standard 6-31G(d,p) basis set. No symmetry constraints were imposed during the optimizations. The stationary points found on the potential energy surfaces as a result of geometry optimizations were tested to represent energy minima rather than saddle points via frequency analysis. The default values for the integration grid (75 radial shells and 302 angular points) and the self-consistent field energy convergence criteria (1×10^{-8}) were used in all calculations. Solvent effects were included by using the integral equation formalism of the polarizable continuum model as implemented in Gaussian 09.[53]

Relaxometric Experiments

For titration experiments, a solution of $ZnCl_2$ of known concentration was added stepwise to a solution of GdL (starting concentration 3.0 mM), and the longitudinal proton relaxation time T_1 was measured after each addition of the analyte. The ^{1}H relaxivity r_1 was calculated from the eq $1/T_{1,obs} = 1/T_{1,d} + r_1 \times [Gd^{3+}]$, where $T_{1,obs}$ is the observed longitudinal relaxation time, $T_{1,d}$ is the diamagnetic contribution in the absence of the paramagnetic substance, and $[Gd^{3+}]$ is the actual concentration of Gd^{3+} at each point of the titration. The initial Gd^{3+} concentrations were determined by measuring the bulk magnetic susceptibility shifts.[54] The concentration of 4-(2-hydroxyethyl)-1-piperazineethanesulfonic acid (HEPES) buffer was 50 mM. The reported values are mean values of three independent experiments.

Competition experiments were performed in a similar fashion. The longitudinal proton relaxation time T_1 was measured for the solution of GdL (starting concentration 3.0 mM) alone, and then after addition of the following solutions: $CaCl_2$, $MgCl_2$, or $CuSO_4$ (2 × 1 equiv). The final values were measured upon addition of $ZnCl_2$ (2 equiv) to these mixtures.

Magnetic Resonance Imaging Experiments

^{1}H MRI was performed on two sets of probes: (1) A solution of GdL (1 mM) to which 0, 0.33, 0.66, and 1 equiv of Zn^{2+} were added; (2) solutions of Dotarem (1 mM) in absence and presence of Zn^{2+} (1 equiv), or water without or with Zn^{2+} (1 mM). These sets were placed in 4 × 200 μL plastic tubes and inserted in the 20 mL syringe filled with water and 162 mM of Dotarem to avoid susceptibility artifacts. ^{1}H T_1 images were acquired using the fast low angle shot pulse sequence: field-of-view = 40 × 40 mm^2, matrix size = 512 × 512, one slice, slice thickness 1 mm, flip angle = 90 ^{o}, echo time = 3.0 ms, repetition time = 60.0 ms, number of averages = 4. The total acquisition time was 1m 1s 440 ms.

Associated Content

Supporting Information

The Supporting Information is available free of charge on the ACS Publications website at DOI: 10.1021/acs.inorgchem.5b01719.

- UV–vis spectra from titration experiments, HR-MS spectra, excitation and emission spectra of TbL, NMR spectra, and optimized Cartesian coordinates obtained with DFT calculations. (PDF)

Author Information

Corresponding Authors

*E-mail: carlos.platas.iglesias@udc.es. (C.P.-I.)

*E-mail: goran.angelovski@tuebingen.mpg.de. (G.A.)

Notes

The authors declare no competing financial interest.

Acknowledgment

We are thankful to T. Savić for performing the MRI experiments. C.P.-I., D.E.-G., and M.R.-F. thank Ministerio de Economía y Competitividad (CTQ2013-43243-P) for generous financial support and Centro de Supercomputación de Galicia (CESGA) for providing the computer facilities. R.T. and V.P. acknowledge the Ministère de l'Enseignement Supérieur et de la Recherche, the Centre National de la Recherche Scientifique. The authors gratefully acknowledge financial support from the Max Planck Society, the Turkish Ministry of Education (Ph.D. fellowship to S.G.), and the COST CM1006 Action "European F-Element Network (EUFEN)". This work is dedicated to Professor Imre Tóth on occasion of his 65th birthday.

References

(1) (a) Andreini, C.; Banci, L.; Bertini, I.; Rosato, A. *J. Proteome Res.* **2006**, 5, 196−201. (b) Lipscomb, W. N.; Sträter, N. *Chem. Rev.* **1996**, 96, 2375−2433.

(2) Lu, J.; Stewart, A. J.; Sleep, D.; Sadler, P. J.; Pinheiro, T. J. T.; Blindauer, C. A. *J. Am. Chem. Soc.* **2012**, 134, 1454−1457.

(3) (a) Frederickson, C. J.; Bush, A. I. *BioMetals* **2001**, 14, 353−366. (b) Qian, W. J.; Gee, K. R.; Kennedy, R. T. *Anal. Chem.* **2003**, 75, 3468−3475. (c) Kolenko, V.; Teper, E.; Kutikov, A.; Uzzo, R. *Nat. Rev. Urol.* **2013**, 10, 219−226.

(4) (a) Franklin, R. B.; Costello, L. C. *J. Cell. Biochem.* **2009**, 106, 750−757. (b) Leal, S. S.; Botelho, H. M.; Gomes, C. M. *Coord. Chem. Rev.* **2012**, 256, 2253−2270.

(5) (a) Kozlowski, H.; Luczkowski, M.; Remelli, M.; Valensin, D. *Coord. Chem. Rev.* **2012**, 256, 2129−2141. (b) Szewczyk, B. *Front. Aging Neurosci.* **2013**, 5, 33.

(6) Bush, A. I.; Tanzi, R. E. *Proc. Natl. Acad. Sci. U. S. A.* **2002**, 99, 7317−7319.

(7) (a) Komatsu, K.; Kikuchi, K.; Kojima, H.; Urano, Y.; Nagano, T. *J. Am. Chem. Soc.* **2005**, 127, 10197−10204. (b) Lim, N. C.; Freake, H. C.; Brückner, C. *Chem. - Eur. J.* **2005**, 11, 38−49.

(8) *The Chemistry of Contrast Agents in Medical Magnetic Resonance Imaging*, 2 ed.; Merbach, A. E., Helm, L., Tóth, É., Eds.; Wiley: Chichester, 2013.

(9) (a) Caravan, P.; Ellison, J. J.; McMurry, T. J.; Lauffer, R. B. *Chem. Rev.* **1999**, 99, 2293−2352. (b) Terreno, E.; Delli Castelli, D.; Viale, A.; Aime, S. *Chem. Rev.* **2010**, 110, 3019−3042. (c) Villaraza, A. J. L.; Bumb, A.; Brechbiel, M. *Chem. Rev.* **2010**, 110, 2921−2959.

(10) (a) Tu, C.; Osborne, E. A.; Louie, A. Y. *Ann. Biomed. Eng.* **2011**, 39, 1335−1348. (b) Hingorani, D. V.; Bernstein, A. S.; Pagel, M. D. *Contrast Media Mol. Imaging* **2015**, 10, 245−265.

(11) de Smet, M.; Heijman, E.; Langereis, S.; Hijnen, N. M.; Grüll, H. *J. Controlled Release* **2011**, 150, 102−110.

(12) (a) Aime, S.; Fedeli, F.; Sanino, A.; Terreno, E. *J. Am. Chem. Soc.* **2006**, 128, 11326−11327. (b) Giovenzana, G. B.; Negri, R.; Rolla, G. A.; Tei, L. *Eur. J. Inorg. Chem.* **2012**, *2012*, 2035−2039.

(13) (a) Tu, C.; Nagao, R.; Louie, A. Y. *Angew. Chem., Int. Ed.* **2009**, 48, 6547−6551. (b) Raghunand, N.; Jagadish, B.; Trouard, T. P.; Galons, J.-P.; Gillies, R. J.; Mash, E. A. *Magn. Reson. Med.* **2006**, 55, 1272−1280.

(14) (a) Chauvin, T.; Durand, P.; Bernier, M.; Meudal, H.; Doan, B.-T.; Noury, F.; Badet, B.; Beloeil, J.-C.; Tóth, É. *Angew. Chem., Int. Ed.* **2008**, 47, 4370−4372. (b) Duimstra, J. A.; Femia, F. J.; Meade, T. J. *J. Am. Chem. Soc.* **2005**, 127, 12847−12855. (c) Urbanczyk-Pearson, L. M.; Femia, F. J.; Smith, J.; Parigi, G.; Duimstra, J. A.; Eckermann, A. L.; Luchinat, C.; Meade, T. J. *Inorg. Chem.* **2008**, 47, 56−68.

(15) (a) Que, E. L.; Chang, C. J. *Chem. Soc. Rev.* **2010**, 39, 51−60. (b) Bonnet, C. S.; Tóth, E. *Future Med. Chem.* **2010**, 2, 367−384.

(16) (a) Hanaoka, K.; Kikuchi, K.; Urano, Y.; Narazaki, M.; Yokawa, T.; Sakamoto, S.; Yamaguchi, K.; Nagano, T. *Chem. Biol.* **2002**, 9, 1027−1032. (b) Hanaoka, K.; Kikuchi, K.; Urano, Y.; Nagano, T. *J. Chem. Soc., Perkin Trans. 2* **2001**, 1840−1843.

(17) (a) Lubag, A. J. M.; De León-Rodríguez, L. M.; Burgess, S. C.; Sherry, A. D. *Proc. Natl. Acad. Sci. U. S. A.* **2011**, 108, 18400−18405. (b) De León-Rodríguez, L. M.; Lubag, A. J. M.; López, J. A.; Andreude-Riquer, G.; Alvarado-Monzón, J. C.; Sherry, A. D. *MedChemComm* **2012**, 3, 480−483. (c) Esqueda, A. C.;

López, J. A.; Andreu-de-Riquer, G.; Alvarado-Monzón, J. C.; Ratnakar, J.; Lubag, A. J. M.; Sherry, A. D.; De León-Rodríguez, L. M. *J. Am. Chem. Soc.* **2009**, 131, 11387−11391.

(18) Rivas, C.; Stasiuk, G. J.; Sae-Heng, M.; Long, N. J. *Dalton Trans.* **2015**, 44, 4976−4985.

(19) Zhang, X.-a.; Lovejoy, K. S.; Jasanoff, A.; Lippard, S. J. *Proc. Natl. Acad. Sci. U. S. A.* **2007**, 104, 10780−10785.

(20) (a) Major, J. L.; Parigi, G.; Luchinat, C.; Meade, T. J. *Proc. Natl. Acad. Sci. U. S. A.* **2007**, 104, 13881−13886. (b) Matosziuk, L. M.; Leibowitz, J. H.; Heffern, M. C.; MacRenaris, K. W.; Ratner, M. A.; Meade, T. J. *Inorg. Chem.* **2013**, 52, 12250−12261. (c) Major, J. L.; Boiteau, R. M.; Meade, T. J. *Inorg. Chem.* **2008**, 47, 10788−10795.

(21) Luo, J.; Li, W.-S.; Xu, P.; Zhang, L.-Y.; Chen, Z.-N. *Inorg. Chem.* **2012**, 51, 9508−9516.

(22) Bonnet, C. S.; Caillé, F.; Pallier, A.; Morfin, J.-F.; Petoud, S.; Suzenet, F.; Tóth, E. *Chem. - Eur. J.* **2014**, 20, 10959−10969.

(23) Stasiuk, G. J.; Minuzzi, F.; Sae-Heng, M.; Rivas, C.; Juretschke, H.-P.; Piemonti, L.; Allegrini, P. R.; Laurent, D.; Duckworth, A. R.; Beeby, A.; Rutter, G. A.; Long, N. J. *Chem. - Eur. J.* **2015**, 21, 5023−5033.

(24) (a) Sarka, L.; Burai, L.; Brücher, E. *Chem. - Eur. J.* **2000**, 6, 719−724. (b) Baranyai, Z.; Brucher, E.; Uggeri, F.; Maiocchi, A.; Toth, I.; Andrasi, M.; Gaspar, A.; Zekany, L.; Aime, S. *Chem. - Eur. J.* **2015**, 21, 4789−4799. (c) Baranyai, Z.; Palinkas, Z.; Uggeri, F.; Maiocchi, A.; Aime, S.; Brucher, E. *Chem. - Eur. J.* **2012**, 18, 16426−16435.

(25) (a) Kallen, A.; Abramova, L.; Saab, G.; Turabelidze, G.; Patel, P.; Arduino, M.; Hess, T.; Cheng, S.; Jhung, M. *Am. J. Kidney Dis.* **2007**, 297, 1542−1544. (b) Darrah, T. H.; Prutsman-Pfeiffer, J. J.; Poreda, R. J.; Campbell, M. E.; Hauschka, P. V.; Hannigan, R. E. *Metallomics* **2009**, 1, 479−488.

(26) Helm, L. *Future Med. Chem.* **2010**, 2, 385−396.

(27) Kadjane, P.; Platas-Iglesias, C.; Boehm-Sturm, P.; Truffault, V.; Hagberg, G. E.; Hoehn, M.; Logothetis, N. K.; Angelovski, G. *Chem. - Eur. J.* **2014**, 20, 7351−7362.

(28) Angelovski, G.; Fouskova, P.; Mamedov, I.; Canals, S.; Tóth, E.; Logothetis, N. K. *ChemBioChem* **2008**, 9, 1729−1734.

(29) Angelovski, G.; Gottschalk, S.; Milosevic, M.; Engelmann, J.; Hagberg, G. E.; Kadjane, P.; Andjus, P.; Logothetis, N. K. *ACS Chem. Neurosci.* **2014**, 5, 360−369.

(30) Gündüz, S.; Nitta, N.; Vibhute, S.; Shibata, S.; Mayer, M. E.; Logothetis, N. K.; Aoki, I.; Angelovski, G. *Chem. Commun.* **2015**, 51, 2782−2785.

(31) Moussaron, A.; Vibhute, S.; Bianchi, A.; Gündüz, S.; Kotb, S.; Sancey, L.; Motto-Ros, V.; Rizzitelli, S.; Crémillieux, Y.; Lux, F.; Logothetis, N. K.; Tillement, O.; Angelovski, G. *Small* **2015**, 11, 4900−4909.

(32) Oukhatar, F.; Meudal, H.; Landon, C.; Logothetis, N. K.; Platas-Iglesias, C.; Angelovski, G.; Tóth, É. *Chem. - Eur. J.* **2015**, 21, 11226−11237.

(33) Roger, M.; Regueiro-Figueroa, M.; Azzeddine, C. B.; Patinec, V.; Bonnet, C. S.; Platas-Iglesias, C.; Tripier, R. *Eur. J. Inorg. Chem.* **2014**, *2014*, 1072−1081.

(34) (a) Roger, M.; Lima, L. M. P.; Frindel, M.; Platas-Iglesias, C.; Gestin, J. F.; Delgado, R.; Patinec, V.; Tripier, R. *Inorg. Chem.* **2013**, 52, 5246−5259. (b) Gasser, G.; Tjioe, L.; Graham, B.; Belousoff, M. J.;

Juran, S.; Walther, M.; Künstler, J. U.; Bergmann, R.; Stephan, H.; Spiccia, L. *Bioconjugate Chem.* **2008**, 19, 719−730. (c) Stavila, V.; Allali, M.; Canaple, L.; Stortz, Y.; Franc, C.; Maurin, P.; Beuf, O.; Dufay, O.; Samarut, J.; Janier, M.; Hasserodt, J. *New J. Chem.* **2008**, 32, 428−435. (d) Weisman, G. R.; Vachon, D. J.; Johnson, V. B.; Gronbeck, D. A. *J. Chem. Soc., Chem. Commun.* **1987**, 886−887.

(35) Horrocks, W. D. W., Jr.; Sudnick, D. *J. Am. Chem. Soc.* **1979**, 101, 334−340.

(36) Beeby, A.; Clarkson, I. M.; Dickins, R. S.; Faulkner, S.; Parker, D.; Royle, L.; de Sousa, A. S.; Williams, J. A. G.; Woods, M. *J. Chem. Soc., Perkin Trans. 2* **1999**, 493−504.

(37) (a) Cacheris, W. P.; Nickle, S. K.; Sherry, A. D. *Inorg. Chem.* **1987**, 26, 958−960. (b) Simecek, J.; Schulz, M.; Notni, J.; Plutnar, J.; Kubicek, V.; Havlickova, J.; Hermann, P. *Inorg. Chem.* **2012**, 51, 577−590.

(38) Kumar, K.; Chang, C. A.; Francesconi, L. C.; Dischino, D. D.; Malley, M. F.; Gougoutas, J. Z.; Tweedle, M. F. *Inorg. Chem.* **1994**, 33, 3567−3575.

(39) Geraldes, C. F. G. C.; Brown, R. D., III; Brucher, E.; Koenig, S. H.; Seymour, H.; Sherry, A. D.; Spiller, M. *Magn. Reson. Med.* **1992**, 27, 284−295.

(40) Congreve, A.; Parker, D.; Gianolio, E.; Botta, M. *Dalton Trans.* **2004**, 1441−1445.

(41) (a) Koullourou, T.; Natrajan, L.; Bhavsar, H.; Pope, S. J. A.; Feng, J.; Narvainen, J.; Shaw, R.; Scales, E.; Kauppinen, R.; Kenwright, A. M.; Faulkner, S. *J. Am. Chem. Soc.* **2008**, 130, 2178−2179. (b) Lowe, M. P.; Parker, D.; Reany, O.; Aime, S.; Botta, M.; Castellano, G.; Gianolio, E.; Pagliarin. *J. Am. Chem. Soc.* **2001**, 123, 7601−7609.

(42) (a) Adair, C.; Woods, M.; Zhao, P.; Pasha, A.; Winter, P. M.; Lanza, G. M.; Athey, P.; Sherry, A. D.; Kiefer, G. E. *Contrast Media Mol. Imaging* **2007**, 2, 55−58. (b) Regueiro-Figueroa, M.; Djanashvili, K.; Esteban-Gomez, D.; Chauvin, T.; Tóth, E.; de Blas, A.; Rodriguez-Blas, T.; Platas-Iglesias, C. *Inorg. Chem.* **2010**, 49, 4212−4223. (c) Polasek, M.; Kotek, J.; Hermann, P.; Cisarova, I.; Binnemans, K.; Lukes, I. *Inorg. Chem.* **2009**, 48, 466−475. (d) Dunand, F. A.; Dickins, R. S.; Parker, D.; Merbach, A. E. *Chem. - Eur. J.* **2001**, 7, 5160−5167. (e) Aime, S.; Botta, M.; Ermondi, G. *Inorg. Chem.* **1992**, 31, 4291−4299.

(43) Regueiro-Figueroa, M.; Esteban-Gómez, D.; de Blas, A.; Rodríguez-Blas, T.; Platas-Iglesias, C. *Chem. - Eur. J.* **2014**, 20, 3974−3981.

(44) Dunand, F. A.; Aime, S.; Geninatti Crich, S.; Giovenzana, G. B.; Merbach, A. E. *Magn. Reson. Chem.* **2002**, 40, 87−92.

(45) Verma, K. D.; Forgacs, A.; Uh, H.; Beyerlein, M.; Maier, M. E.; Petoud, S.; Botta, M.; Logothetis, N. K. *Chem. - Eur. J.* **2013**, 19, 18011−18026.

(46) Wilcox, C. S. *Frontiers in Supramolecular Chemistry and Photochemistry*; VCH: Weinheim, Germany, 1991; pp 123−143.

(47) (a) Cortes, S.; Brucher, E.; Geraldes, C. F. G. C.; Sherry, A. D. *Inorg. Chem.* **1990**, 29, 5−9. (b) Bevilacqua, A.; Gelb, R. I.; Hebard, W. B.; Zompa, L. J. *Inorg. Chem.* **1987**, 26, 2699−2706.

(48) Que, E. L.; Gianolio, E.; Baker, S. L.; Wong, A. P.; Aime, S.; Cheng, C. J. *J. Am. Chem. Soc.* **2009**, 131, 8527−8536.

(49) Livramento, J. B.; Weidensteiner, C.; Prata, M. I. M.; Allegrini, P. R.; Geraldes, C. F. G. C.; Helm, L.; Kneuer, R.; Merbach, A. E.; Santos, A. C.; Schmidt, P.; Tóth, E. *Contrast Media Mol. Imaging* **2006**, 1, 30−39.

(50) Frisch, M. J.; Trucks, G. W.; Schlegel, H. B.; Scuseria, G. E.; Robb, M. A.; Cheeseman, J. R.; Scalmani, G.; Barone, V.; Mennucci, B.; Petersson, G. A.; Nakatsuji, H.; Caricato, M.; Li, X.; Hratchian, H. P.; Izmaylov, A. F.; Bloino, J.; Zheng, G.; Sonnenberg, J. L.; Hada, M.; Ehara, M.; Toyota, K.; Fukuda, R.; Hasegawa, J.; Ishida, M.; Nakajima, T.; Honda, Y.; Kitao, O.; Nakai, H.; Vreven, T.; Montgomery, J. A., Jr.; Peralta, J. E.; Ogliaro, F.; Bearpark, M.; Heyd, J. J.; Brothers, E.; Kudin, K. N.; Staroverov, V. N.; Kobayashi, R.; Normand, J.; Raghavachari, K.; Rendell, A.; Burant, J. C.; Iyengar, S. S.; Tomasi, J.; Cossi, M.; Rega, N.; Millam, N. J.; Klene, M.; Knox, J. E.; Cross, J. B.; Bakken, V.; Adamo, C.; Jaramillo, J.; Gomperts, R.; Stratmann, R. E.; Yazyev, O.; Austin, A. J.; Cammi, R.; Pomelli, C.; Ochterski, J. W.; Martin, R. L.; Morokuma, K.; Zakrzewski, V. G.; Voth, G. A.; Salvador, P.; Dannenberg, J. J.; Dapprich, S.; Daniels, A. D.; Farkas, Ö.; Foresman, J. B.; Ortiz, J. V.; Cioslowski, J.; Fox, D. J. *Gaussian 09*, Revision A.01; Gaussian, Inc: Wallingford, CT, 2009.

(51) Tao, J. M.; Perdew, J. P.; Staroverov, V. N.; Scuseria, G. E. *Phys. Rev. Lett.* **2003**, 91, 146401.

(52) Dolg, M.; Stoll, H.; Savin, A.; Preuss, H. *Theor. Chim. Acta* **1989**, 75, 173−194.

(53) Tomasi, J.; Mennucci, B.; Cammi, R. *Chem. Rev.* **2005**, 105, 2999−3093.

(54) Corsi, D. M.; Platas-Iglesias, C.; van Bekkum, H.; Peters, J. A. *Magn. Reson. Chem.* **2001**, 39, 723−726.